LYMPHATIC RESEARCH AND BIOLOGY
Volume 12, Number 4, 2014

DOI: 10.1089/lrb.2014.0012

Radiation-Induced Impairment in Lung Lymphatic Vasculature

Ye Cui, MD, PhD,[1] Julie Wilder, PhD,[2] Cecilia Rietz, PhD,[2] Andrew Gigliotti, DVM, PhD,[2] Xiaomeng Tang, MS,[2] Yuanyuan Shi, PhD,[2] Raymond Guilmette, PhD,[2] Hao Wang, BS,[1] Gautam George, MD,[1] Eduarda Nilo de Magaldi,[1] Sarah G. Chu, MD,[1] Melanie Doyle-Eisele, PhD,[2] Jacob D. McDonald, PhD,[2] Ivan O. Rosas, MD,[1,2] and Souheil El-Chemaly, MD, MPH[1,2]

Abstract

Background: The lymphatic vasculature has been shown to play important roles in lung injury and repair, particularly in lung fibrosis. The effects of ionizing radiation on lung lymphatic vasculature have not been previously reported.

Methods and Results: C57Bl/6 mice were immobilized in a lead shield exposing only the thoracic cavity, and were irradiated with a single dose of 14 Gy. Animals were sacrificed and lungs collected at different time points (1, 4, 8, and 16 weeks) following radiation. To identify lymphatic vessels in lung tissue sections, we used antibodies that are specific for lymphatic vessel endothelial receptor 1 (LYVE-1), a marker of lymphatic endothelial cells (LEC). To evaluate LEC cell death and oxidative damage, lung tissue sections were stained for LYVE-1 and with TUNEL staining, or 8-oxo-dG respectively. Images were imported into ImageJ v1.36b and analyzed. Compared to a non-irradiated control group, we observed a durable and progressive decrease in the density, perimeter, and area of lymphatic vessels over the study period. The decline in the density of lymphatic vessels was observed in both subpleural and interstitial lymphatics. Histopathologically discernible pulmonary fibrosis was not apparent until 16 weeks after irradiation. Furthermore, there was significantly increased LEC apoptosis and oxidative damage at one week post-irradiation that persisted at 16 weeks.

Conclusions: There is impairment of lymphatic vasculature after a single dose of ionizing radiation that precedes architectural distortion and fibrosis, suggesting important roles for the lymphatic circulation in the pathogenesis of the radiation-induced lung injury.

Introduction

Radiation therapy is an essential treatment modality for multiple malignancies, such as lung and breast cancer.[1,2] Despite recent technical advances in radiation therapy, incidental irradiation that damages normal lung tissue in the path of the radiation beam remains unavoidable and frequently results in radiation-induced lung injury (RILI).[3] As such, this deleterious pulmonary effect not only compromises quality of life for a subset of long-term cancer survivors but also represents a major dose-limiting factor in radiation therapy.[4]

The sequential damage following RILI begins with an acute phase of pneumonitis and culminates in a chronic stage of lung fibrosis.[5] Although the dynamic histopathologic features of RILI appear to be well characterized, the exact cellular and molecular processes remain enigmatic and somewhat controversial. The prevailing hypothesis holds that the interactions of alveolar epithelial cells, inflammatory cells, and fibroblasts are primarily responsible for the pathogenesis of RILI.[6–8] On the other hand, the roles of other cell types present in the lung, including lymphatic endothelial cells (LECs) have received less attention.

LECs line the inner surface of the lymphatic network in which lymph flows unidirectionally toward the heart. A functioning lymphatic system plays a pivotal role in mediating tissue homeostasis by resorbing fluid, macromolecules, and cells from the interstitial space.[9] Conversely, aberrant lymphatic development or injury to lymphatic vessels can lead to gradual accumulation of interstitial fluid and

[1]Division of Pulmonary and Critical Care Medicine, Brigham and Women's Hospital, Harvard Medical School, Boston, Massachusetts.
[2]Lovelace Respiratory Research Institute, Albuquerque, New Mexico.

ultimately connective tissue remodeling.[10] One of the most common causes of lymphatic injury is radiation therapy.[11] Observational studies conducted over the past several decades have shown an association between radiation exposure and reduced lymphatic drainage.[12–14] At the cellular level, it has recently been demonstrated that radiation may cause severe dermal lymphatic dysfunction through augmenting dermal LEC apoptotic cell death in a mouse tail model.[13]

Pulmonary lymphatics are particularly important for maintaining alveolar clearance, which is required for efficient gas exchange at the alveolar–capillary barrier.[15] Lymphatic abnormalities have been previously reported in idiopathic pulmonary fibrosis (IPF).[16–19] In addition, studies have shown that in an animal model of lung fibrosis, impeding lymphatic drainage leads to worsening fibrotic changes.[20] However, to date, the effects of radiation on lung lymphatics have not been explored. Here, we investigated the effects of a single dose of radiation on lung lymphatic vasculature and their temporal relationship to the development of fibrosis.

Material and Methods

Animal experiments

All animal experimental procedures were approved by the Institutional Animal Care and Use Committee at Lovelace Respiratory Research Institute. Briefly, female C57Bl/6 mice (9–11 weeks of age) were anesthetized and immobilized under a lead shield exposing only the thoracic cavity. Animals were irradiated with a single dose of 14 Gy delivered by a Philips X-ray Therapy Unit (Philips, Andover, MA). Radiated and age-matched non-irradiated control animals ($n = 3$ per group per time point) were sacrificed at one, 4, 8, and 16 weeks post-exposure.

Antibodies

A complete list of antibodies used in this study is provided in Table 1.

Immunohistochemistry and immunofluorescence

Formalin-fixed, paraffin-embedded tissue sections obtained from radiated and non-irradiated control lungs were analyzed. Sections were deparaffinized in xylene and rehydrated through a graded series of ethanol, followed by antigen retrieval with citrate buffer (pH 6.0) for 20 min at 95°C. To identify lymphatic vessels in tissue sections, antibodies that are specific for lymphatic vessel endothelial hyaluronan receptor 1 (LYVE-1) and for vascular endothelial growth factor receptor (VEGFR)-3, markers of lymphatic endothelial cells, were used.[21,22] To detect the expression of lymphangiogeneic growth factors, tissue sections from the indicated time point were also incubated with anti-VEGF-C and VEGF-D. To identify blood vessel endothelial cells and areas of fibrosis, anti-VEGFR-2 and anti-S100A4 antibodies were used respectively.[22,23] Sections were incubated with the primary antibody or an isotype control in a humidified chamber overnight at 4°C. Sections were then incubated with appropriate secondary antibodies using a HRP-DAB Cell & Tissue Staining Kit (R&D Systems, Minneapolis, MN) according to manufacturer's instructions. Sections were then briefly counterstained with hematoxylin.

To measure radiation-induced oxidative stress in LECs *in vivo*, anti-8-oxo-7,8-dihydro-2'-deoxyguanosine (8-oxo-dG) staining was performed.[24] Briefly, sections were soaked in 2 N HCl for 5 min to denature DNA and neutralized in 1 M Tris-base for 5 min at room temperature. After blocking for 1 h with 10% normal goat serum in phosphate buffer saline (PBS), sections were incubated in the mixture of 8-oxo-DG and LYVE-1 antibodies or appropriate isotype controls in a humidified chamber at 4°C overnight, followed by a mixture of two secondary antibodies (Alexa Fluor 594 goat anti-mouse IgG and Alexa Fluor 488 goat anti-rabbit IgG) for 1 h at room temperature in the dark. Slides were then mounted using mounting medium containing 4,6-diamidino-2-phenylindole-2-HCl (DAPI) (Vector Laboratories Inc., Burlingame, CA).

To detect *in vivo* cell apoptosis, terminal deoxynucleotidyl transferase dUTP nick end labeling (TUNEL) staining[25] was performed using the In Situ Cell Death Detection kit, TMR red (Roche Applied Science, Indianapolis, IN) according to manufacturer's recommendations. To localize LECs, sections were then incubated with anti-LYVE-1 antibodies. Reactions were detected using Alexa Fluor 488 goat anti-rabbit IgG. In addition, positive (DNase I treatment) and negative controls (label solution only) for TUNEL staining and negative controls for LYVE-1 staining with non-immune rabbit IgG were performed in parallel.

Microscopy and image analysis

Tissue sections incubated with anti–LYVE-1, anti-VEGFR-2, or anti-VEGFR-3 antibodies were inspected using wide-field microscopy with an Olympus FSX-100 microscope (Olympus, Center Valley, PA). Multiple photomicrographs were captured and stitched to create panoramic images of entire tissue sections. For immunofluorescence staining, images from five random fields containing lymphatic vessels were obtained per animal using an Olympus FV-10i confocal laser scanning microscope (Olympus).

Images were imported into ImageJ v1.36b (National Institutes of Health, http://rsbweb.nih.gov/ij/). The differentially immunostained lymphatic and blood vessels were identified and manually traced. The density of lymphatic or

Table 1. List of Antibodies Used

LYVE-1	Immunohistochemistry Immunofluorescence	Catalog no. 11-034, (AngioBio, Del Mar, CA)
S100A4	Immunohistochemistry	Catalog no. ab27957, (Abcam, Cambridge, MA)
VEGF-C	Immunohistochemistry	Catalog no. ab9546, (Abcam)
VEGF-D	Immunohistochemistry	Catalog no. sc-25784, (Santa Cruz, Dallas, Texas)
VEGFR-2	Immunohistochemistry	Catalog no. ab51873, (Abcam)
VEGFR-3	Immunohistochemistry	Catalog no. AF743, (R&D Systems)
8-oxo-dG	Immunofluorescence	Catalog no. 4354-MC-050, (Trevigen, Gaithersburg, MD)

blood vessels is expressed as the total number of lymphatic or blood vessels in the entire tissue divided by the area of the entire tissue. The diameters, cross-sectional areas, and perimeter were subsequently quantified. Numbers of TUNEL/LYVE-1-positive and 8-oxo-dG/LYVE-1-positve cells were counted in a blinded fashion. The number of double-positive cells per field was divided by the perimeter of lymphatic vessels in the same field for normalization.

Mean linear intercept

To evaluate the structural alterations in mouse lung following radiation exposure, we measured mean linear intercept (MLI) according to methods described previously.[26] Briefly, five random non-overlapping fields of lung tissue per animal devoid of major airways and vasculature were digitally photographed at 200× magnification, and ten equally spaced horizontal lines were superimposed on these captured photomicrographs. MLI was calculated by dividing the length of the grid line by the number of intersections with alveolar walls. The MLI values were then averaged to obtain a single value for each sample.

Statistical analysis

Data were presented as mean ± SEM. Statistical analysis was performed using Student's *t*-tests to analyze the differences between irradiated and non-irradiated groups. Multiple comparisons were evaluated by one way analysis of variance (ANOVA) followed by Tukey's *post hoc* test. Analyses were performed using GraphPad Prism 5.0 (GraphPad Software, San Diego, CA). A two-tailed p value of <0.05 was considered significant.

Results

Persistent loss of mouse lung lymphatic vessels after a single dose of ionizing radiation

To assess the effects of a single dose of radiation on lymphatic vessels, mouse lung tissue sections from indicated time points post radiation exposure or age-matched control mice were immunostained with anti-LYVE-1 antibodies. In non-irradiated normal mouse lung tissue, lymphatic vessels reactive with anti-LYVE-1 antibodies were found dispersed throughout the lung parenchyma (Fig. 1A, C). In marked contrast, we observed a decrease in the numbers of LYVE-1 positive lymphatic vessels as early as one week post-irradiation, when cellular infiltration and architectural distortion of the lung were not visible by light microscopic examination (Fig. 1B).

As expected, at 16 weeks post-irradiation (Fig. 1D and Supplementary Fig. S1), histologic evaluation showed thickened alveolar walls accompanied by an increase in the number of alveolar macrophages throughout the lung tissue and distinct multifocal patches of fibrosis (identified with anti-S100A4 antibodies) predominantly within the subpleural lung parenchyma. Interestingly, and consistent with previous reports,[16,17] we noticed a relative lack of lymphatic vessels in areas of dense fibrosis.

The number, perimeter, and area of lymphatic vessels were quantified and subsequently adjusted to the cross sectional area of the entire digitally reconstituted tissue (Supplementary Fig. S2). Our data showed that compared to control lungs, lungs from radiated mice demonstrated a significant decrease in the density, perimeter, and area of lymphatic vessels (Fig. 1E, F, and G, respectively) at 1 week post-irradiation ($p<0.05$). Importantly, these changes were persistent and remained significant at 16 weeks post-irradiation with greater than 75% reduction in density, area, and perimeter of lymphatic vessels compared to age-matched controls. These data indicated a durable and progressive effect of a single dose of ionizing radiation on lung LECs.

Since LYVE-1 could be affected by inflammation and is not exclusive to the lymphatic circulation,[27,28] we performed immunohistochemical analysis of mouse lung from weeks 1 and 16 with anti-VEGFR-3 antibodies (Supplementary Fig. S3). Consistent with the results obtained with anti-LYVE-1 antibodies, VEGFR-3 immunostaining showed a decrease in lymphatic vessel density in radiated lungs as early as week 1, which was persistent at week 16.

Radiation-induced changes in lymphatic vessels observed in the subpleural and interstitial compartments

To better understand the distribution patterns of pulmonary lymphatic vessels, we divided lung tissue into either subpleural or interstitial compartments (Fig. 2A, B). Our results showed that changes in lymphatic vessel density were observed as early as 1 week post-irradiation in both subpleural and interstitial compartments (Fig. 2C, F). Additionally, the decline in perimeter and area of interstitial lymphatic vessels (Fig. 2G, H) was already apparent 1 week post-radiation compared to control non-irradiated mice, whereas subpleural lymphatic perimeter and area were similar to control mice at this time point (Fig. 2D, E). Radiation-induced changes in both subpleural and interstitial lymphatic vessels were persistent at 16 weeks compared to the control lungs (Fig. 2C–H). Additionally, morphometric analysis confirmed that there was no significant difference in mean linear intercept (MLI) between control and radiated mice at week 1 and week 16 (Supplementary Fig. S4), indicating that changes in lymphatic vessel density and size were not related to lung inflation conditions or variations in alveolar airspaces.

Age-related increase in lung lymphatic vessel area and perimeter

In non-irradiated lung tissue, there was a modest but insignificant increase in the density of LYVE-1 positive lymphatic vessels over the 16-week study period (Fig. 3A, D, G), during which the density of VEGFR-3 positive lymphatic vessels increased significantly (Supplementary Fig. 3E). In addition, adult mice (6 months of age) showed a significant increase in the perimeter and area ratio of lung lymphatic vessels when compared to juvenile mice (2 months of age) (Fig. 3B, C). This increase in perimeter and area ratio of lymphatic vessels was primarily driven by changes in the interstitial lymphatics (Fig. 3H, I), since no significant changes in subpleural lymphatics (Fig. 3E, F) were observed over the 16-week study period.

Transient induction of angiogenesis in mouse lung after a single dose of ionizing radiation

Angiogenesis and lymphangiogenesis play important roles in inflammation, tissue injury, and repair.[29–31] Previous studies have shown that radiation therapy promotes the formation

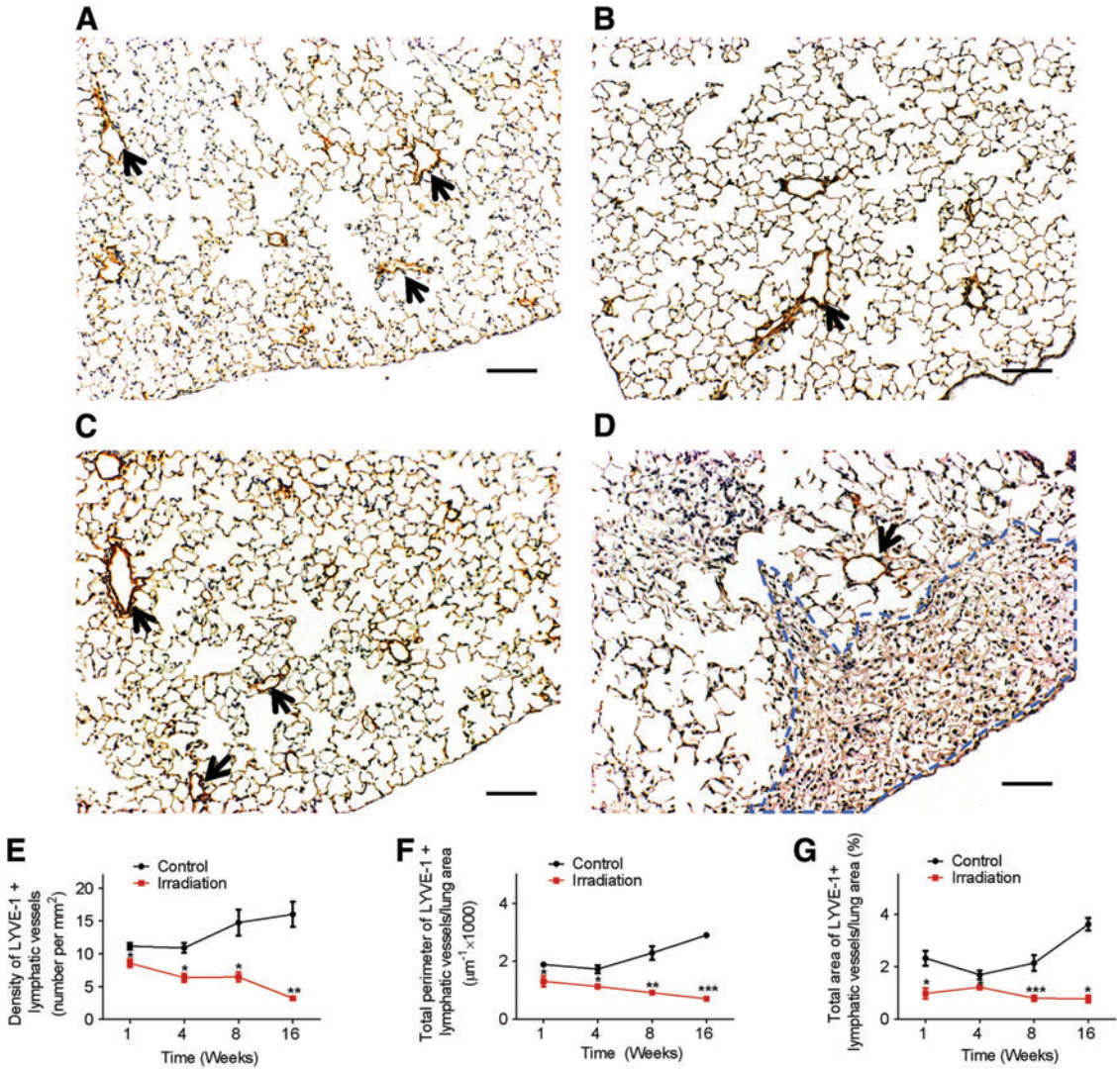

FIG. 1. Decrease in lymphatic vessels after a single dose of radiation. One week after a single dose (14 Gy) of radiation, radiated lungs **(B)** show a marked decrease in immunoreactivity with anti-LYVE-1 antibodies (*brown areas indicated by black arrows*) compared to control nonradiated lungs **(A)**. At 16 weeks post-radiation, the decrease in immunoreactivity with anti-LYVE-1 antibodies persisted as seen in lung tissue sections from nonradiated **(C)** and radiated animals **(D)**. Areas of fibrosis (**D**, enclosed in *blue dotted lines*) observed 16 weeks after radiation were completely devoid of lymphatic vessels. (Scale bar: 100 μm). Images of the entire lung section were obtained. ImageJ software was used to measure the density, area, and perimeter of lymphatic vessels in tissue sections from radiated and control animals at the indicated time points ($n = 3$ per group per time point). A statistically significant decrease in lymphatic vessel density **(E)**, perimeter **(F)**, and area **(G)** was observed; $*p < 0.05$; $**p < 0.01$; $***p < 0.001$, compared to time-matched controls by Student t test. A color version of this figure is available in the online article at www.liebertpub.com/lrb.

of new blood vessels in both preclinical animal models and in skin samples from breast cancer patients.[32,33] To examine changes in the blood vasculature after radiation exposure, mouse lung tissue sections were immunostained with anti-VEGFR-2 antibodies. Blood vessels immunoreactive with anti-VEGFR-2 antibodies were quantified at two different time points (Fig. 4). In non-irradiated lung tissue at 1 and 16 weeks (Fig. 4A, C, respectively), blood capillaries were present throughout the lung tissue and particularly in the alveolar septa. As early as 1 week after radiation exposure, we observed an increase in the number of microvessels in the lung parenchyma (Fig. 4B, E). This increase in angiogenesis was transient, however, with subsequent microvessel density decreasing to baseline levels at 16 weeks (Fig. 4D, E).

Radiation is associated with increased lung LECs apoptosis

In view of the decreased lung lymphatics following radiation exposure, we hypothesized that radiation induces lung LEC apoptosis. To this end, we performed a dual labeling with TUNEL and anti-LYVE-1 antibodies in mouse lung tissue. Apoptotic LECs were rarely observed in non-irradiated control lungs at 1 and 16 weeks (Fig. 5A, B). In contrast, we found that as early as 1 week post-irradiation, there was markedly

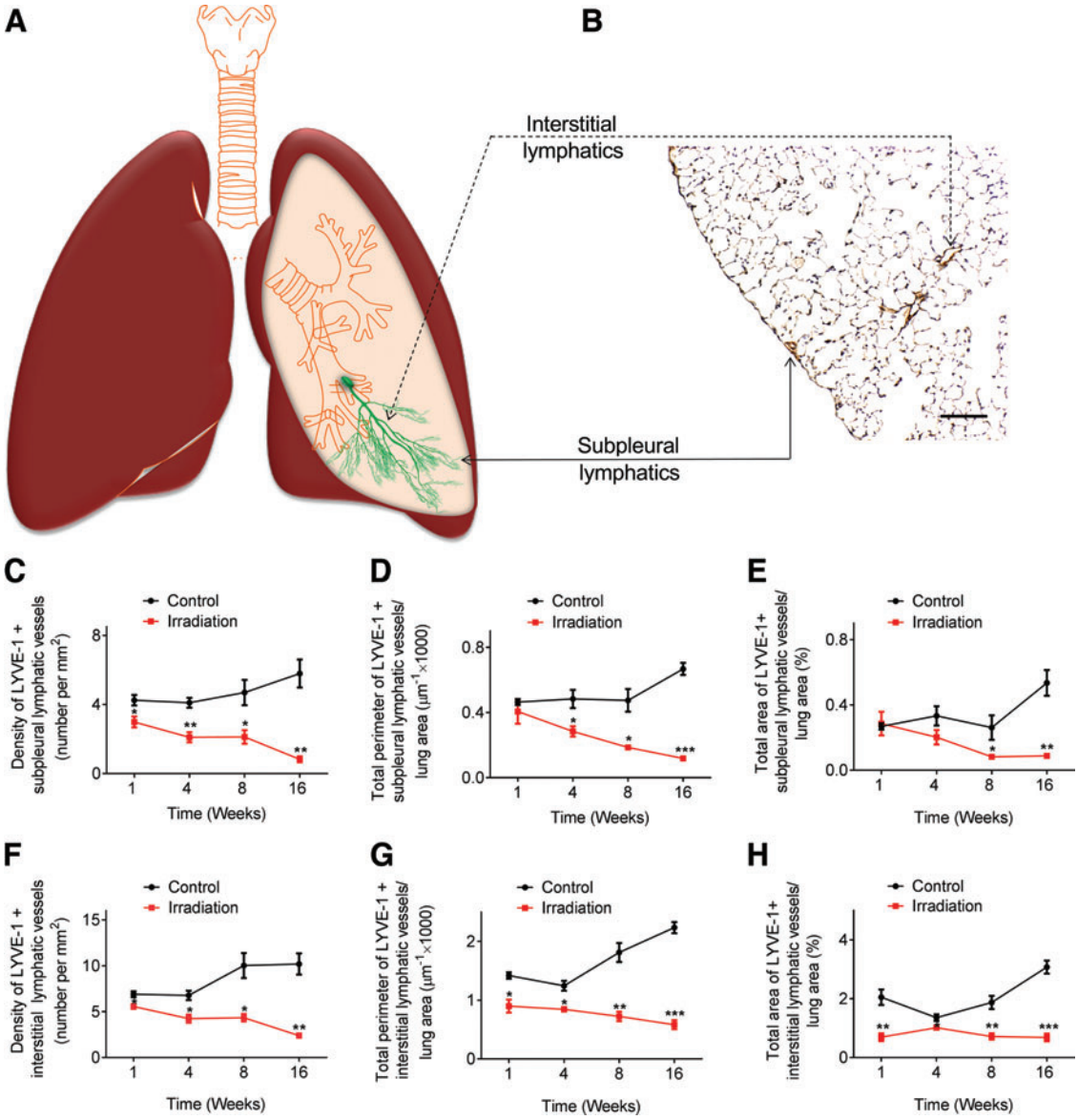

FIG. 2. Morphometric analysis of lymphatic vessels in the subpleural and interstitial compartments. Schematic representation of subpleural and interstitial lymphatics **(A)**. Lung tissue sections showing immunoreactivity with anti-LYVE-1 antibodies, with subpleural and interstitial lymphatic vessels highlighted in **(B)**. (Scale bar: 100 μm). Significant changes in subpleural lymphatic density **(C)**, perimeter **(D)**, and area **(E)** were observed at the indicated time points following radiation exposure. Changes in interstitial lymphatic density **(F)**, perimeter **(G)**, and area **(H)** were observed as early as one week post-radiation ($n = 3$ mice per group per time point); $*p < 0.05$; $**p < 0.01$; $***p < 0.001$, compared to time-matched controls by Student t test. A color version of this figure is available in the online article at www.liebertpub.com/lrb.

increased LEC apoptosis in the radiated lungs. This increase in LEC apoptosis was persistent at 16 weeks following irradiation (Fig. 5B, C).

Persistent increase in oxidative stress in lung LECs after a single dose of ionizing radiation

Accumulating evidence suggests that reactive oxygen species (ROS) and the resulting cellular redox imbalance are pivotal in regulating apoptosis.[34,35] Additionally, excessive cellular ROS production has been observed immediately following radiation exposure, with increasing apoptotic cell death as a consequence.[36,37] Here, we explored the possibility that pulmonary lymphatic endothelium could be a potential target for radiation-induced oxidative stress. We conducted double immunofluorescence staining for 8-oxo-dG and LYVE-1 in mouse lung sections. 8-Oxo-dG is one of the mutagenic base modifications generated by ROS. It is a sensitive and frequently used marker for oxidative stress.[24]

Similar to the patterns seen in TUNEL staining, quantification of 8-oxo-dG/LYVE-1 double positive cells showed significantly increased levels of oxidative stress in LECs in mouse lung at 1 week (Fig. 6A, C) and 16 weeks (Fig. 6B, C) post-irradiation compared to non-irradiated controls.

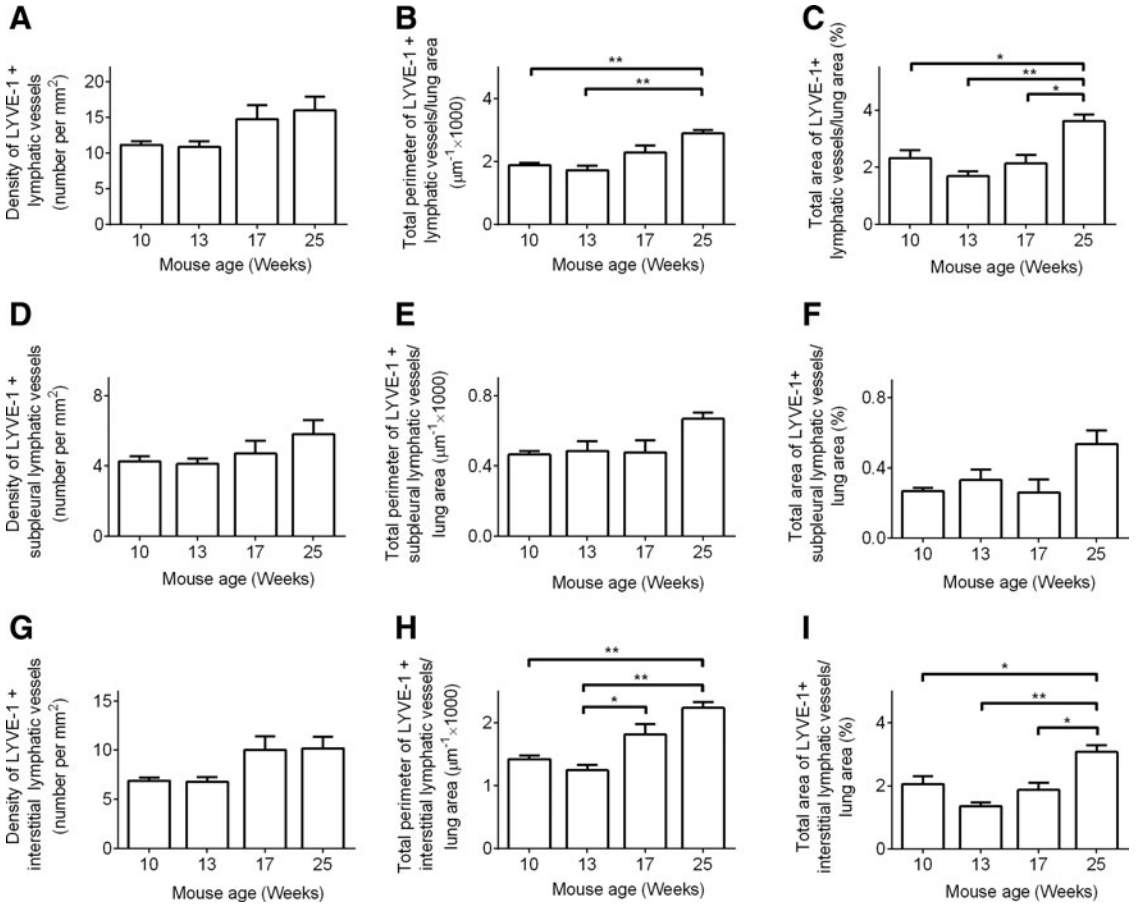

FIG. 3. Age-related changes in lymphatic vessels. 9-week-old mice were allowed to age. Lung tissues were collected at indicated time points, and lymphatic vessels were identified with anti-LYVE-1 antibodies. Images of the entire lung section were obtained. ImageJ software was used to measure the density **(A, D**, and **G)**, perimeter **(B**, **E**, and **H)**, and area **(C**, **F**, and **I)** of total **(A–C)**, subpleural **(D–F)**, and interstitial **(G–I)** lymphatic vessels in lung tissue sections at the indicated time points ($n = 3$ per group per time point). Results showed that between 10 weeks and 25 weeks of age, there was no significant change in total, subpleural, or interstitial lymphatic vessel density **(A, D**, and **G)**. Throughout the study period, there was no significant change in subpleural lymphatic vessel perimeter **(E)** or area **(F)**. A statistically significant age-related increase in the perimeter **(B** and **H)** and area ratio **(C** and **I)** of total and interstitial lymphatic vessels was observed; $*p < 0.05$; $**p < 0.01$, by 1-way ANOVA. (These data are different representations of the same data from control animals in Figs. 1 and 2. These graphs are meant to illustrate the maturation effects on lung lymphatic vessels).

Expression patterns of VEGF-C and VEGF-D are altered in response to radiation

Within the VEGF family, VEGF-C and -D constitute a functional subgroup that orchestrates lymphatic vasculature development.[38] To explore whether they are modulated in RILI, we stained consecutive cut mouse lung sections with antibodies against VEGF-C and –D and examined their distribution patterns. VEGF-C and -D were predominantly observed in epithelial cells and alveolar macrophages in both control (Fig. 7A, C) and radiated lungs (Fig. 7B, D). Notably, there were increased numbers of VEGF-C and –D positive alveolar macrophages despite the significant decrease in lymphatic vessels associated with radiation exposure. Additionally, fibrotic lesions in the radiated mouse lung exhibited strong immunoreactivity for VEGF-C (Fig. 7B) and relatively weak immunoreactivity for VEGF-D (Fig. 7D), whereas VEGF-D was abundantly expressed within interstitial cells in non-irradiated control lungs (Fig. 7C). No staining was observed when the primary antibodies were replaced by normal rabbit IgG (Fig. 7E, F).

Conclusions

Nearly a century after the identification of two separate types of RILI (an acute phase of pneumonitis and a chronic stage of lung fibrosis),[39] there are no studies to date that have systematically examined the effects of radiation on pulmonary lymphatics. In the present study, we provide the first comprehensive analysis of the lymphatic vasculature in a RILI mouse model and demonstrate that radiation exposure leads to early-onset and progressive loss of pulmonary lymphatic vessels. Changes to the lymphatic circulation preceded any significant structural alterations in the lung, suggesting a role for the lymphatic circulation in the development of RILI.

Over the study period, changes in density, area, and perimeter were found in both the subpleural and interstitial lymphatics, which share similar functions. However, the direction of the lymph flow differs, with subpleural lymphatics draining towards the pleura, and interstitial lymphatics draining towards the hilum. Furthermore, subpleural lymphatics are significantly more efficient in fluid drainage.[40]

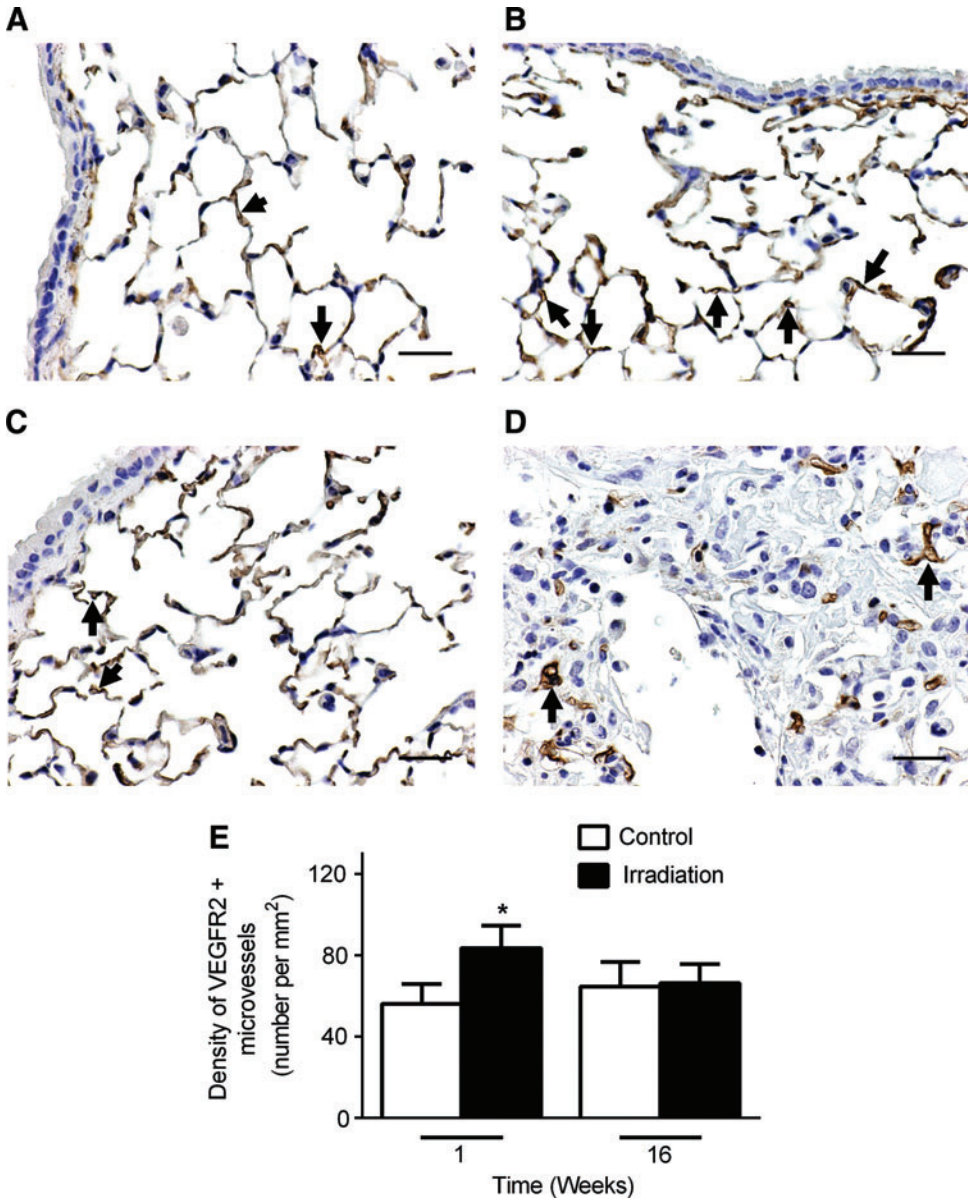

FIG. 4. Transient increase in blood capillaries after one dose of radiation. Lung tissue sections were immunostained with anti-VEGFR-2 antibodies (*black arrows*) to visualize blood capillaries. One week after a single dose of radiation, VEGFR-2 positive blood capillaries were increased **(B)** compared to control nonradiated lungs **(A)**. At 16 weeks there were no significant differences in VEFGR-2 positive (*black arrows*) blood capillary density in nonradiated **(C)** compared to radiated lungs **(D)**. Clusters of irregularly shaped capillaries were observed along the periphery of fibrotic lesions but were virtually absent in the fibrotic areas **(D)**. (Scale bar: 25 μm). **(E)** Images of the entire lung section were obtained. ImageJ software was used to calculate the density of VEGFR-2 positive blood capillaries in tissue sections from radiated and control animals at the indicated time points ($n = 3$ per group per time point); $^*p < 0.05$, compared to time-matched controls by Student t test. A color version of this figure is available in the online article at www.liebertpub.com/lrb.

Whether these observations play important roles in the development of pulmonary fibrosis—a predominantly subpleural disease—remain to be investigated.

Previous studies on human idiopathic pulmonary fibrosis (IPF) have shown that there is an increase in lymphatic vessels with worsening fibrosis,[16,20,41,42] which contradicts our present findings. However, most recent evidence suggests that these newly formed lymphatic vessels in IPF are not functional either because of fragmentation[17] or mural cells that block lymphatic drainage,[20] the net effect being impaired lymphatic function in human fibrotic lung disease.

Several murine models have been developed to decipher the pathogenesis of IPF. Among these, intratracheal instillation of bleomycin remains the most widely utilized approach to induce experimental lung fibrosis. Nevertheless, the bleomycin model does not sufficiently recapitulate the pathological and clinical features of human IPF.[43] In particular, 1) bleomycin induces bronchiolocentric fibrotic changes, whereas changes in IPF are predominantly peripheral and subpleural; 2) the reversibility of fibrotic changes in the bleomycin model versus the progressive nature of human IPF; and 3) the rapid transition from injury to the fibrotic phase in the bleomycin model

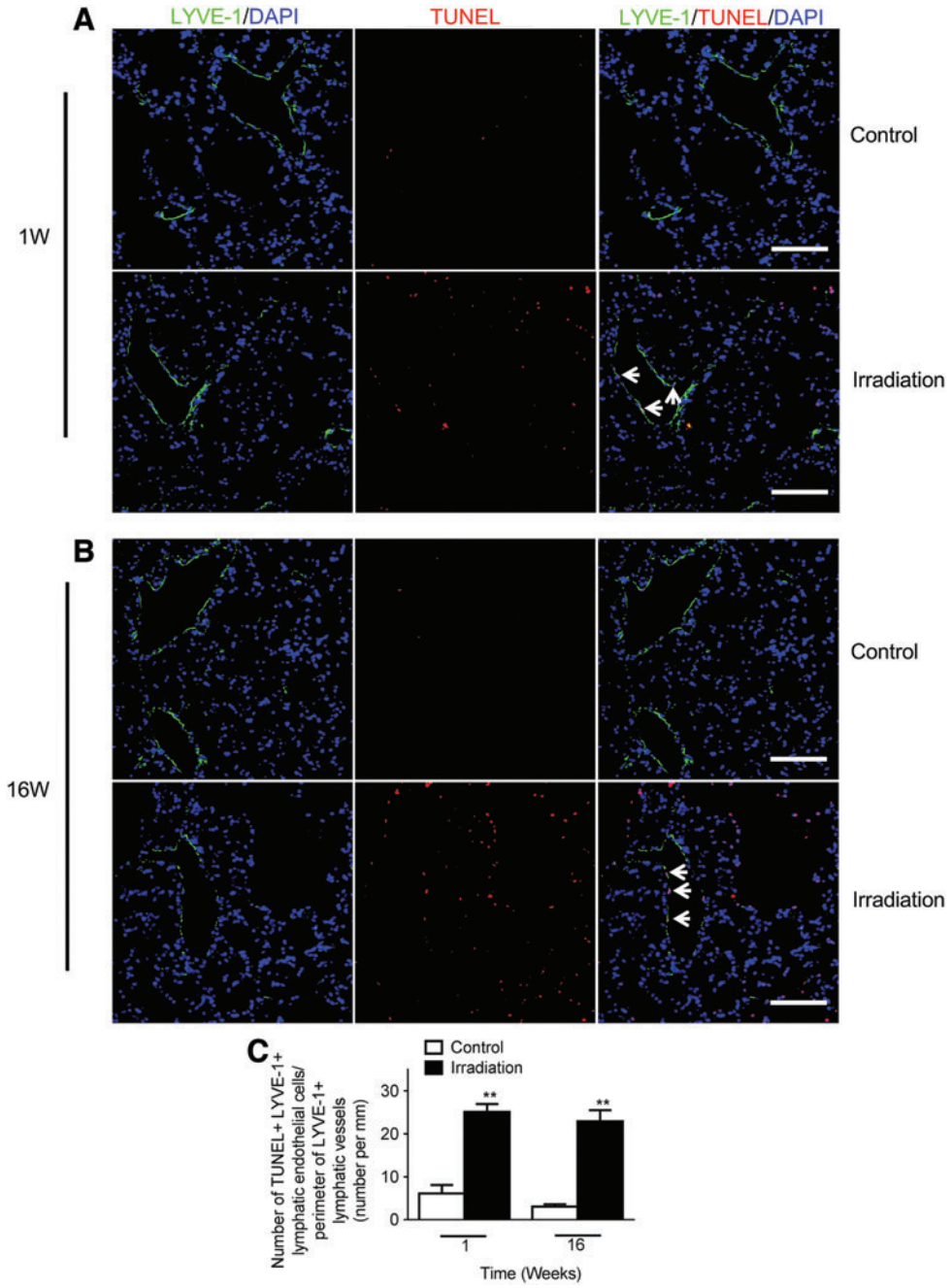

FIG. 5. Increased lymphatic endothelial cell death after single dose radiation. Representative images of lymphatic vessels (LYVE-1, *green*), and terminal deoxynucleotidyl transferase-mediated dUTP nick-end labeling (TUNEL, *red*) staining of lung tissue from control and radiated lungs at one **(A)** and 16 weeks **(B)** after a single dose of radiation (14 Gy). Nuclei were counterstained with 4',6-diamidino-2-phenylindole (DAPI). (Scale bar: 100 μm). **(C)** Apoptotic cell index calculated as the number of TUNEL positive/LYVE-1 positive lymphatic endothelial cells (indicated by *white arrows* in the merged images in **A** and **B**) per field divided by the perimeter of lymphatic vessels in the same field. There was a significant increase in lymphatic endothelial cell apoptosis at one and 16 weeks in radiated versus control lungs ($n = 3$ mice per group per time point); $^{**}p < 0.01$, compared to time-matched controls by Student t test. A color version of this figure is available in the online article at www.liebertpub.com/lrb.

(measured in days) versus the chronic condition of human IPF that spans many years.[44,45] The radiation model we used is characterized by pronounced fibrotic changes in the lung by 16 weeks post-exposure of the thorax to a single radiation dose.[46] In addition, the radiation induced lung fibrosis model more closely mimics human IPF in regard to the peripheral distribution of fibrotic changes and the time frame for fibrosis development (measured in months).[47]

Previous research has shown that radiation exposure induces production of free radicals, activates redox signaling,[36] and compromises the capacity of the antioxidant defense system in the lung.[48] As a result, the imbalance between ROS

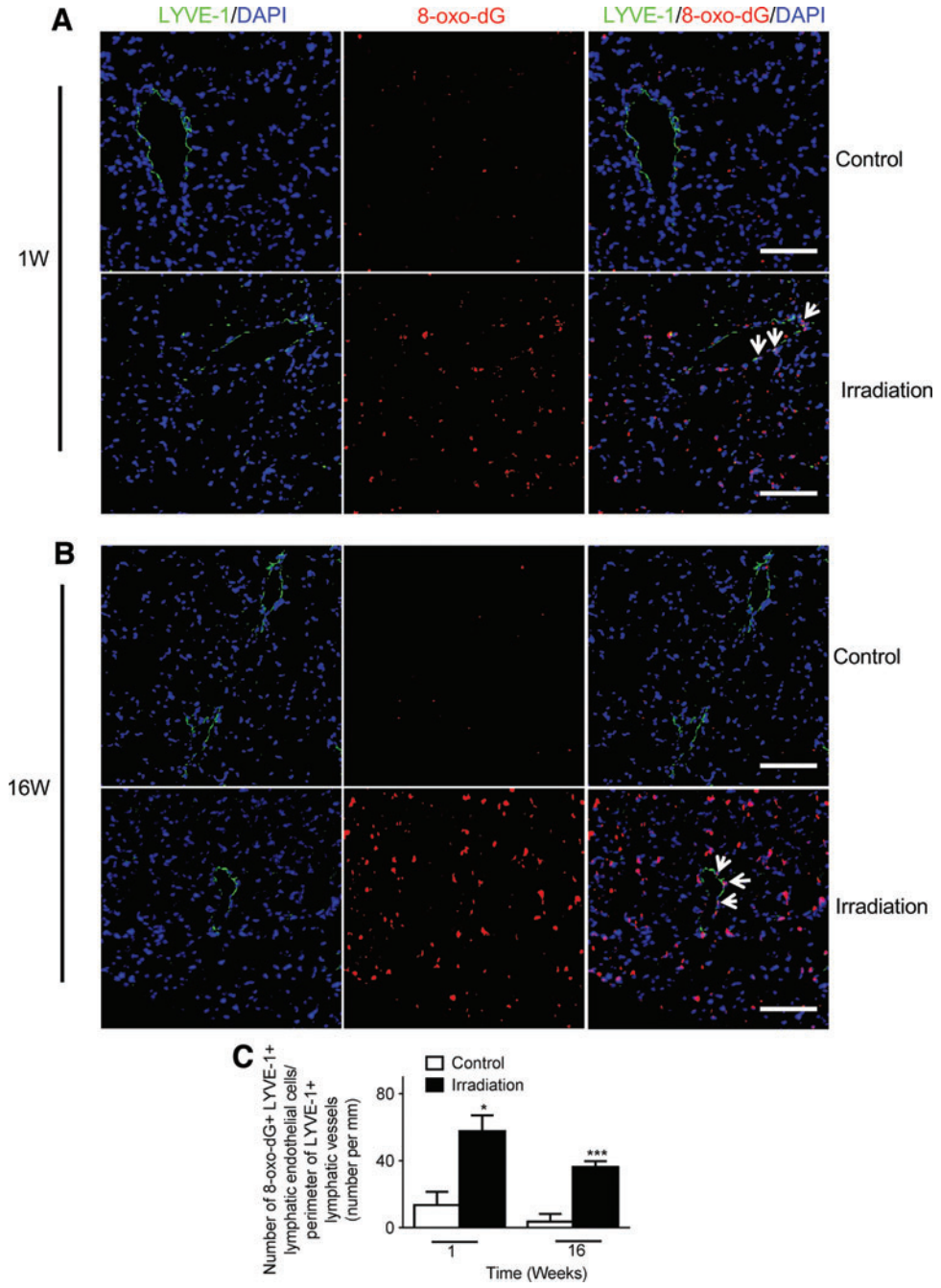

FIG. 6. Increased lung lymphatic vessel oxidative damage after single dose of radiation. Representative images of lymphatic vessels (LYVE-1, *green*) and 8-oxo-dG (8-oxo-dG, *red*) staining of lung tissue sections from control and radiated lungs at one **(A)** and 16 **(B)** weeks after a single dose radiation (14 Gy). Nuclei were counterstained with 4',6-diamidino-2-phenylindole (DAPI). (Scale bar: 100 μm). **(C)** The number of 8-oxo-dG positive/LYVE-1 positive lymphatic endothelial cells per field (*white arrows* in the merged images in **A** and **B**) was divided by the perimeter of lymphatic vessels in the same field. There was a significant increase in oxidative stress at one and 16 weeks post radiation ($n = 3$ per group per time point); $*p < 0.05$; $***p < 0.001$, compared to time-matched controls by Student t test. A color version of this figure is available in the online article at www.liebertpub.com/lrb.

production and scavenging elicits enhanced oxidative stress and may lead to DNA damage. Indeed, we observed a concomitant increase in the markers of oxidative stress and apoptosis in the pulmonary lymphatic endothelium in our animal model, which could explain, at least in part, the gradual depletion of lymphatic vessels post radiation exposure. Findings of this study are also supported by recent observations that radiation induces loss of dermal lymphatic vessels through its pro-apoptotic effect on dermal LECs.[13] In contrast to these reports, an earlier study demonstrates that LECs from small intestine and peri-tumoral regions are resistant to apoptosis following whole-body irradiation.[49] The

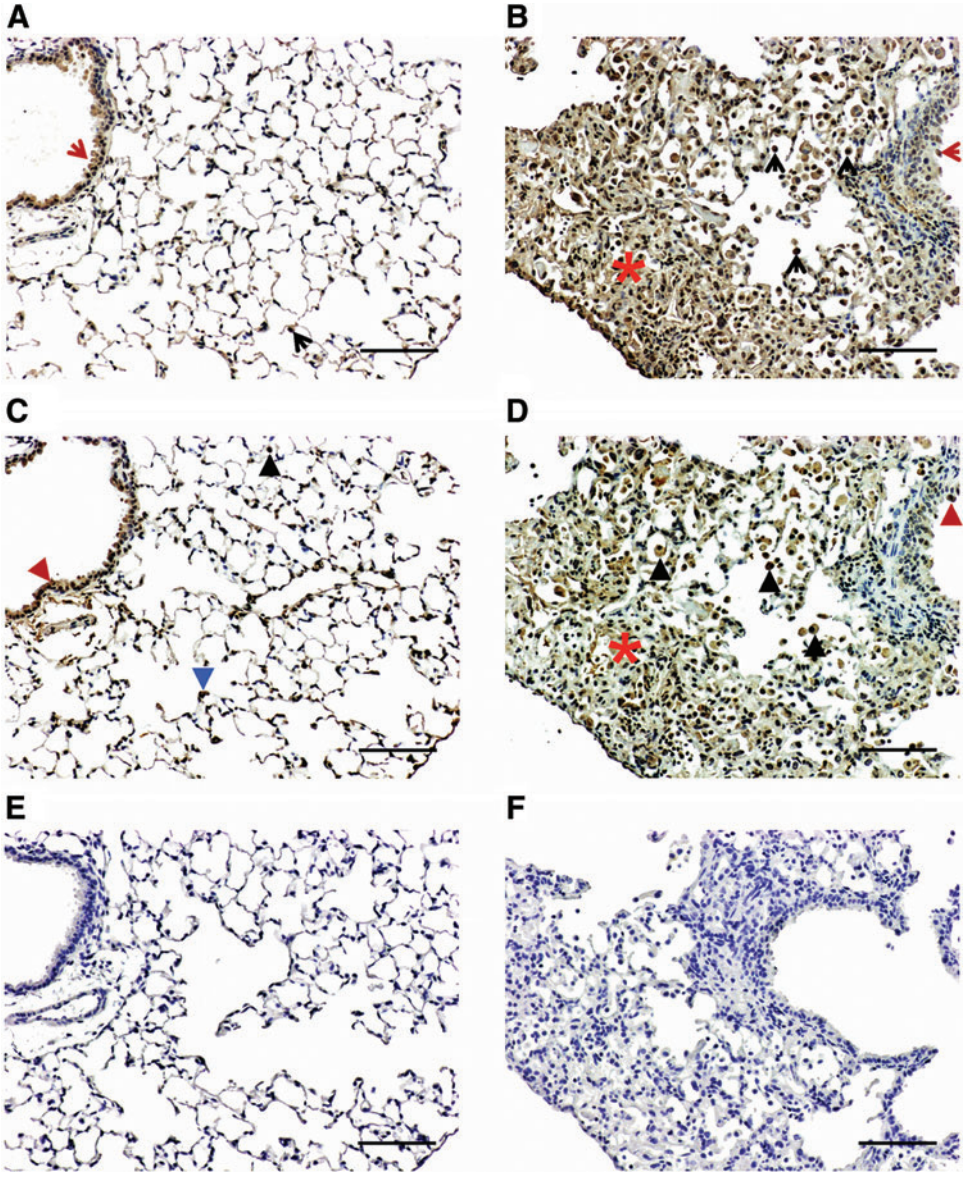

FIG. 7. Immunoreactive VEGF-C and VEGF-D in control and radiated lungs. Representative images of VEGF-C **(A** and **B)** and VEGF-D **(C** and **D)** immunostaining visualized with diaminobenzidine (DAB) at 16 weeks post-irradiation. VEGF-C immunoreactivity was observed in epithelial cells (*red arrow*) and alveolar macrophages (*black arrow*) in both control **(A)** and radiated lungs **(B)**. VEGF-D immunoreactivity was observed in epithelial cells (*red arrowhead*) and alveolar macrophages (recognized by their morphology and presence in the alveolar space; *black arrowhead*) in both control **(C)** and radiated lungs **(D)**. Fibrotic areas in the radiated mouse lung (*red asterisk*) exhibited immunoreactivity for VEGF-C **(B)** and relatively weak immunoreactivity for VEGF-D **(D)**, whereas VEGF-D was expressed within interstitial cells in control lungs (identified by their localization at the basal membrane side of alveolar epithelial cells, *blue arrowhead*, **C**). No staining was observed when primary antibodies were replaced with normal IgG **(E** and **F)**. (Scale bar: 100 μm). A color version of this figure is available in the online article at www.liebertpub.com/lrb.

cause for this potential contradiction is not clear, although it might simply reflect the variations of radiosensitivity among LECs from different organs and tissues. Of particular relevance to our current findings, ROS have been shown to mediate the activation of transforming growth factor (TGF)-β1,[50] which is a critical regulator of both acute and chronic RILI.[51–53]

It is well established that VEGF-C and –D are required to sustain postnatal lymphatic development.[9,54] We observed a marked increase in the number of VEGF-C and -D positive alveolar macrophages in radiated mouse lung. This increase was apparently insufficient to induce lymphatic regeneration. Consistent with the present results, previous studies have demonstrated that upregulation of VEGF-C fails to promote lymphangiogenesis during wound healing.[55,56] A possible explanation for the above findings might be that these lymphangiogenic stimuli are overpowered by the abundant presence of anti-lymphangiogenic factors such as activated TGF-β1, which is known to suppress the expression of Prox-1, a critical regulator of lymphangiogenesis.[57–59]

Several recent studies have examined changes in the lymphatic circulation that relate to normal physiological aging.[60–63] This long-term study allowed us to examine age-related changes in lung lymphatic vasculature. We noted an increase in the density, perimeter, and area of pulmonary lymphatics over the 16-week study period. These alterations in lung lymphatic vessels could be parts of the normal physiological changes associated with maturation process.

Although the endothelia of blood and lymphatic vessels share similar properties, they have acquired distinct structural and functional characteristics and are regulated in different fashions.[10] Consistent with published literature,[33] the results of our study indicate that radiation exposure is associated with an early and transient increase in blood vessels, which could be partially attributed to the proangiogenic effects of oxidative stress.[64] Although further investigation is warranted, the opposite findings in blood and lymphatic vessels suggest that radiation and oxidative stress may generate cell type-specific responses. Additionally, our findings support the notion that unlike blood vessels, alterations of lymphatic vessels are generally irreversible.[65]

In conclusion, there is an early-onset and progressive loss of pulmonary lymphatic vasculature with radiation exposure. Mouse lung LECs are susceptible to radiation-induced oxidative stress and apoptosis. Our results suggest that lymphatic vessels are not only tightly connected to the aberrant remodeling process, but could play important roles in the pathogenesis of radiation-induced lung injury and repair. Further studies are needed to investigate the effects of modulating lymphangiogenesis in RILI.

Author Disclosure Statement

No competing financial interests exist.

References

1. Rengan R, Maity AM, Stevenson JP, Hahn SM. New strategies in non-small cell lung cancer: Improving outcomes in chemoradiotherapy for locally advanced disease. Clinical Cancer Research 2011;17:4192–4199.
2. Ragaz J, Olivotto IA, Spinelli JJ, Phillips N, Jackson SM, Wilson KS, Knowling MA, Coppin CM, Weir L, Gelmon K, Le N, Durand R, Coldman AJ, Manji M. Locoregional radiation therapy in patients with high-risk breast cancer receiving adjuvant chemotherapy: 20-year results of the British Columbia randomized trial. J Natl Cancer Instit 2005;97:116–126.
3. Ghafoori P, Marks LB, Vujaskovic Z, Kelsey CR. Radiation-induced lung injury. Assessment, management, and prevention. Oncology 2008;22:37–47; discussion 52–33.
4. Williams JP, Johnston CJ, Finkelstein JN. Treatment for radiation-induced pulmonary late effects: Spoiled for choice or looking in the wrong direction? Current Drug Targets 2010;11:1386–1394.
5. Cappuccini F, Eldh T, Bruder D, Gereke M, Jastrow H, Schulze-Osthoff K, Fischer U, Kohler D, Stuschke M, Jendrossek V. New insights into the molecular pathology of radiation-induced pneumopathy. Radiother Oncol 2011; 101:86–92.
6. Almeida C, Nagarajan D, Tian J, leal SW, Wheeler K, Munley M, Blackstock W, Zhao W. The role of alveolar epithelium in radiation-induced lung injury. PloS one. 2013;8:e53628.
7. Hill RP, Zaidi A, Mahmood J, Jelveh S. Investigations into the role of inflammation in normal tissue response to irradiation. Radiother Oncol 2011;101:73–79.
8. Tada H, Ogushi F, Tani K, Nishioka Y, Miyata JY, Sato K, Asano T, Sone S. Increased binding and chemotactic capacities of PDGF-BB on fibroblasts in radiation pneumonitis. Radiat Res 2003;159:805–811.
9. Schulte-Merker S, Sabine A, Petrova TV. Lymphatic vascular morphogenesis in development, physiology, and disease. J Cell Biol 2011;193:607–618.
10. Choi I, Lee S, Hong YK. The new era of the lymphatic system: No longer secondary to the blood vascular system. Cold Spring Harbor Persp Med 2012;2:a006445.
11. Hinrichs CS, Watroba NL, Rezaishiraz H, Giese W, Hurd T, Fassl KA, Edge SB. Lymphedema secondary to postmastectomy radiation:Incidence and risk factors. Ann Surg Oncol 2004;11:573–580.
12. Mortimer PS, Simmonds RH, Rezvani M, Robbins ME, Ryan TJ, Hopewell JW. Time-related changes in lymphatic clearance in pig skin after a single dose of 18 Gy of X rays. Br J Radiol 1991;64:1140–1146.
13. Avraham T, Yan A, Zampell JC, Daluvoy SV, Haimovitz-Friedman A, Cordeiro AP, Mahrara BJ. Radiation therapy causes loss of dermal lymphatic vessels and interferes with lymphatic function by TGF-beta1-mediated tissue fibrosis. Am J Physiol Cell Physiol 2010;299:C589–605.
14. Baker A, Semple JL, Moore S, Johnston M. Lymphatic function is impaired following irradiation of a single lymph node. Lymph Res Biol 2014;12:76–88.
15. Lauweryns JM, Baert JH. Alveolar clearance and the role of the pulmonary lymphatics. Am Rev Respir Dis 1977; 115:625–683.
16. El-Chemaly S, Malide D, Zudaire E, Ikeda Y, Weinberg BA, Pacheco-Rodriguez G, Rosas IO, Aparicio M, Renn P, MacDonald SD, Wu HP, Nathan SD, Cuttitta F, McCoy JP, Gochuico BR, and Moss J. Abnormal lymphangiogenesis in idiopathic pulmonary fibrosis with insights into cellular and molecular mechanisms. Proc Natl Acad Sci USA 2009;106: 3958–3963.
17. Ebina M, Shibata N, Ohta H. The disappearance of subpleural and interlobular lymphatics in idiopathic pulmonary fibrosis. Lymphat Res Biol 2010;8:199–207.
18. El-Chemaly S, Pacheco-Rodriguez G, Ikeda Y, Malide D, Moss J. Lymphatics in idiopathic pulmonary fibrosis: New insights into an old disease. Lymphat Res Biol 2009;7:197–203.
19. Glasgow CG, El-Chemaly S, Moss J. Lymphatics in lymphangioleiomyomatosis and idiopathic pulmonary fibrosis. Eur Respir Rev 2012;21:196–206.
20. Meinecke AK, Nagy N, Lago GD, Kirmse S, Klose R, Schrodter K, Zimmermann A, Helfrich I, Rundqvist H, Theegarten D, Anhenn O, Orian-Rousseau V, Johnson RS, Alitalo K, Fischer JW, Fandrey J, Stockmann C. Aberrant mural cell recruitment to lymphatic vessels and impaired lymphatic drainage in a murine model of pulmonary fibrosis. Blood 2012;119:5931–5942.
21. Podgrabinska S, Braun P, Velasco P, Kloos B, Pepper MS, Skobe M. Molecular characterization of lymphatic endothelial cells. Proc Natl Acad Sci USA 2002;99:16069–16074.
22. Baluk P, McDonald DM. Markers for microscopic imaging of lymphangiogenesis and angiogenesis. Ann NY Acad Sci 2008;1131:1–12.

23. Lawson WE, Polosukhin VV, Zoia O, Stathopoulos GT, Han W, Plieth D, Loyd JE, Neilson EG, Blackwell TS. Characterization of fibroblast-specific protein 1 in pulmonary fibrosis. Am J Respir Crit Care Med 2005;171:899–907.
24. Haghdoost S, Czene S, Naslund I, Skog S, Harms-Ringdahl M. Extracellular 8-oxo-dG as a sensitive parameter for oxidative stress in vivo and in vitro. Free Rad Res 2005; 39:153–162.
25. Gavrieli Y, Sherman Y, Ben-Sasson SA. Identification of programmed cell death in situ via specific labeling of nuclear DNA fragmentation. J Cell Biol 1992;119:493–501.
26. Robbesom AA, Versteeg EM, Veerkamp JH, van Krieken JH, Bulten HJ, Smits HT, Willems LN, van Herwaarden CL, Dekhuijzen PN, van Kuppevelt TH. Morphological quantification of emphysema in small human lung specimens: comparison of methods and relation with clinical data. Mod Pathol 2003;16:1–7.
27. Johnson LA, Prevo R, Clasper S, Jackson DG. Inflammation-induced uptake and degradation of the lymphatic endothelial hyaluronan receptor LYVE-1. J Biol Chem 2007;282:33671–33680.
28. Mouta Carreira C, Nasser SM, di Tomaso E, Padera TP, Boucher Y, Tomarev SI, Jain RK. LYVE-1 is not restricted to the lymph vessels: Expression in normal liver blood sinusoids and down-regulation in human liver cancer and cirrhosis. Cancer Res 2001;61:8079–8084.
29. Jackson JR, Seed MP, Kircher CH, Willoughby DA, Winkler JD. The codependence of angiogenesis and chronic inflammation. FASEB J 1997;11:457–465.
30. Halin C, Detmar M. Chapter 1. Inflammation, angiogenesis, and lymphangiogenesis. *Methods in Enzymology*. New York: Academic Press; 2008:1–25.
31. Zgraggen S, Ochsenbein AM, Detmar M. An important role of blood and lymphatic vessels in inflammation and allergy. J Allergy 2013;2013:672381.
32. Moeller BJ, Cao Y, Li CY, Dewhirst MW. Radiation activates HIF-1 to regulate vascular radiosensitivity in tumors: role of reoxygenation, free radicals, and stress granules. Cancer Cell 2004;5:429–441.
33. Jackowski S, Janusch M, Fiedler E, Marsch WC, Ulbrich EJ, Gaisbauer G< Dunst J, Kerjaschki D, Helmbold P. Radiogenic lymphangiogenesis in the skin. Am J Pathol 2007;171:338–348.
34. Trachootham D, Lu W, Ogasawara MA, Nilsa RD, Huang P. Redox regulation of cell survival. Antioxid Redox Signal 2008;10:1343–1374.
35. Circu ML, Aw TY. Reactive oxygen species, cellular redox systems, and apoptosis. Free Rad Biol Med 2010;48:749–762.
36. Leach JK, Van Tuyle G, Lin PS, Schmidt-Ullrich R, Mikkelsen RB. Ionizing radiation-induced, mitochondria-dependent generation of reactive oxygen/nitrogen. Cancer Res 2001;61:3894–3901.
37. Zhang Y, Zhang X, Rabbani ZN, Jackson IL, Vujaskovic Z. Oxidative stress mediates radiation lung injury by inducing apoptosis. Intl J Radiat Oncol Biol Phys 2012;83:740–748.
38. Achen MG, Jeltsch M, Kukk E, Makinen T, Vitali A, Wilks AF, Alitalo K, Stacker SA. Vascular endothelial growth factor D (VEGF-D) is a ligand for the tyrosine kinases VEGF receptor 2 (Flk1) and VEGF receptor 3 (Flt4). Proc Natl Acad Sci USA 1998;95:548–553.
39. Evans W, Leucutia T. Intrathoracic changes induced by heavy irradiation. AJR 1925;13:203.
40. Schraufnagel DE. Lung lymphatic anatomy and correlates. Pathophysiology 2010;17:337–343.
41. Lara AR, Cosgrove GP, Janssen WJ, Huie TJ, Burnham EL, Heinz DE, Curran-Everett D, Sahin H, Schwarz MI, Cool CD, Groshong SD, Geraci MW, Tuder RM, Hyde DM, Henson PM. Increased lymphatic vessel length is associated with the fibroblast reticulum and disease severity in usual interstitial pneumonia and nonspecific interstitial pneumonia. Chest 2012;142:1569–1576.
42. Parra ER, Araujo CA, Lombardi JG, Ab'Saver AM, Carvalho CR, Kairalla RA, Capelozzi VL. Lymphatic fluctuation in the parenchymal remodeling stage of acute interstitial pneumonia, organizing pneumonia, nonspecific interstitial pneumonia and idiopathic pulmonary fibrosis. Braz J Med Biol Res 2012;45:466–472.
43. Moore B, Lawson WE, Oury TD, Sisson TH, Raghavendran K, Hogaboam CM. Animal models of fibrotic lung disease. Am J Respir Cell Mol Biol 2013;49:167–179.
44. Scotton CJ, Chambers RC. Bleomycin revisited: Towards a more representative model of IPF? Am J Physiol Lung Cell Molecular Physiol 2010;299:L439–441.
45. Chua F, Gauldie J, Laurent GJ. Pulmonary fibrosis: Searching for model answers. Am J Respir Cell Mol Biol 2005;33:9–13.
46. Puthawala K, Hadjiangelis N, Jacoby SC, Bayongan E, Zhao Z, Yang Z, Devitt ML, Horan GS, Weinreb PH, Lukashev ME, Violette SM, Grant KS, Colarossi C, Formenti SC, Munger JS. Inhibition of integrin alpha(v)beta6, an activator of latent transforming growth factor-beta, prevents radiation-induced lung fibrosis. Am J Respir Crit Care Med 2008;177:82–90.
47. Moore BB, Hogaboam CM. Murine models of pulmonary fibrosis. Am J Physiol Lung Cell Mol Physiol 2008;294: L152–160.
48. Ao X, Lubman DM, Davis MA, Xing X, Kong FM, Lawrence TS, Zhang M. Comparative proteomic analysis of radiation-induced changes in mouse lung: fibrosis-sensitive and -resistant strains. Radiat Res 2008;169:417–425.
49. Sung HK, Morisada T, Cho CH, Oike Y, Lee J, Sung EK, Chung JH, Suda T, Koh GY. Intestinal and peri-tumoral lymphatic endothelial cells are resistant to radiation-induced apoptosis. Biochem Biophys Res Commun 2006;345: 545–551.
50. Cui Y, Robertson J, Maharaj S, waldhauser L, Niu J, wanag J, Farkas L, Kolb M, Gauldie J. Oxidative stress contributes to the induction and persistence of TGF-beta1 induced pulmonary fibrosis. Intl J Biochem Cell Biol 2011;43: 1122–1133.
51. Yi ES, Bedoya A, Lee H, Chin E, Sauanders W, Kim SJ, Danielpour D, Remick DG, Yin S, Ulich TR. Radiation-induced lung injury in vivo: Expression of transforming growth factor-beta precedes fibrosis. Inflammation 1996;20:339–352.
52. Vujaskovic Z, Groen HJ. TGF-beta, radiation-induced pulmonary injury and lung cancer. Intl J Radiat Biol 2000; 76:511–516.
53. Flechsig P, Dadrich M, Bickelhaupt S, Jenne J, Hauser K, Timke C, Peschke P, Hahn EW, Grone HJ, Yingling J, Lahn M, Wirkner U, Huber PE. LY2109761 attenuates radiation-induced pulmonary murine fibrosis via reversal of TGF-beta and BMP-associated proinflammatory and proangiogenic signals. Clin Cancer Res 2012;18:3616–3627.
54. Karpanen T, Wirzenius M, Makinen T, Veikkola T, Haisma HJ, Achen MG, Stacker SA, Pytowski B, Tla-Herttuala S, Alitalo K. Lymphangiogenic growth factor responsiveness is modulated by postnatal lymphatic vessel maturation. Am J Pathol 2006;169:708–718.

55. Goldman J, Le TX, Skobe M, Swartz MA. Overexpression of VEGF-C causes transient lymphatic hyperplasia but not increased lymphangiogenesis in regenerating skin. Circ Res 2005;96:1193–1199.
56. Rutkowski JM, Moya M, Johannes J, Goldman J, Swartz MA. Secondary lymphedema in the mouse tail: Lymphatic hyperplasia, VEGF-C upregulation, and the protective role of MMP-9. Microvasc Res 2006;72:161–171.
57. Clavin NW, Avraham T, Fernandez J, Daluvoy SV, Soares MA, Chaudhry A, Mehrara BJ. TGF-beta1 is a negative regulator of lymphatic regeneration during wound repair. Am J Physiol Heart Circ Physiol 2008;295:H2113–2127.
58. Cui Y, Osorio JC, Risquez C, Wang H, Shi Y, Gochuico BR, Morse D, Rosas IO, EL-Chemaly S. Transforming growth factor-beta1 downregulates vascular endothelial growth factor-D expression in human lung fibroblasts via JNK signaling pathway. Mol Med 2014;20:120–134.
59. Oka M, Iwata C, Suzuki HI, Kiyono K, Morishita Y, Watabe T, Komuro A, Kano MR, Miyazono K. Inhibition of endogenous TGF-beta signaling enhances lymphangiogenesis. Blood 2008;111:4571–4579.
60. Gashev AA, Zawieja DC. Hydrodynamic regulation of lymphatic transport and the impact of aging. Pathophysiology 2010;17:277–287.
61. Thangaswamy S, Bridenbaugh EA, Gashev AA. Evidence of increased oxidative stress in aged mesenteric lymphatic vessels. Lymphat Res Biol 2012;10:53–62.
62. Bridenbaugh EA, Nizamutdinova IT, Jupiter D, Nagai T, Thangaswamy S, Chatterjee V, Gashev AA. Lymphatic muscle cells in rat mesenteric lymphatic vessels of various ages. Lymphat Res Biol 2013;11:35–42.
63. Gashev AA, Chatterjee V. Aged lymphatic contractility: Recent answers and new questions. Lymphat Res Biol 2013; 11:2–13.
64. Yasuda M, Ohzeki Y, Shimizu S, Naaito S, Ohtsuru A, Yamamoto T, Kurosawa Y. Stimulation of in vitro angiogenesis by hydrogen peroxide and the relation with ETS-1 in endothelial cells. Life Sci 1999;64:249–258.
65. Baluk P, Tammela T, Ator E, Lyubynska N, Achen MG, Hicklin DJ, Jeltsch M, Petrova TV, Pytowski B, Stacker SA, Yla-Herttuala S, Jackson DG, Alitalo K, McDonald DM. Pathogenesis of persistent lymphatic vessel hyperplasia in chronic airway inflammation. J Clin Invest 2005; 115:247–257.

Address correspondence to:
Souheil El-Chemaly, MD, MPH
Division of Pulmonary and Critical Care Medicine
Brigham and Women's Hospital
75 Francis Street
Boston, MA 02115

E-mail: sel-chemaly@partners.org